OFFPRINTS FROM NEURAL CONTROL OF RHYTHMIC MOVEMENTS IN VERTEBRATES
Edited by Dr. Avis Cohen

Chapter Nine

SYSTEMS OF COUPLED OSCILLATORS AS MODELS OF CENTRAL PATTERN GENERATORS

RICHARD H. RAND
AVIS H. COHEN
PHILIP J. HOLMES

Department of Theoretical and Applied Mechanics
Section of Neurobiology and Behavior
Cornell University
Ithaca, New York

1 INTRODUCTION

In the development of the mathematical framework that follows, we are motivated by three major goals. The first is to construct models which will allow us to test assertions regarding the structure and function of the intersegmental coordinating system of the lamprey central pattern generator (CPG) for locomotion (Cohen and Wallén, 1980; see Grillner et al., Chapt. 1, for the description of the motor pattern). In the process, we hope, secondly, to formulate some general concepts which might be useful in understanding other biological systems of coupled oscillators. Finally, we will formulate a method for analysis of CPGs. In view of these considerations, we have allowed the lamprey experimental data to guide our thinking while at the same time emphasizing those aspects of the dynamical behav-

ior of the models which should be shared by a rather general class of systems. In some instances we sacrifice considerable physiological and anatomical detail in order to obtain tractability of the equations or generality of the model. While a general theory is still far from complete, in this chapter we offer some basic results we have obtained. During the course of the discussion, we point out the relevant relations to the lamprey as well as draw analogies with other CPGs to which the model might be applied. In her chapter, Kopell further develops these ideas. She also develops the mathematics which is required for the changes and provides additional examples of the usefulness of the models.

The mathematics used both in our chapter and in that of Kopell requires some knowledge of advanced calculus, linear algebra, and differential equations. It is not expected to be easily accessible to mathematically inexperienced readers. However, we will attempt to relate the ideas to biological systems represented elsewhere in the book in hopes of motivating the biologist to seek an applied mathematician with whom to collaborate. Generally, we have tried to separate the biological and mathematical components of the discussion. The mathematical treatments will begin with a description of the biological significance of the assumptions and will end with conclusions again placed in a biological context. Unfortunately, some jargon is unavoidable, and some terms must be used which are impossible to define adequately in a few words. However, these can often be finessed

FIGURE 1. A system of N oscillators with nearest neighbor interactions.

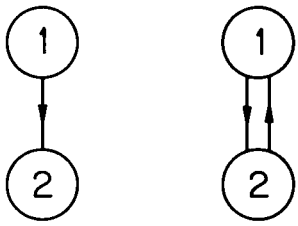

17 **FIGURE 2.** One-way coupling versus two-way coupling.

by the reader and the general meaning can still be derived. We encourage this approach. *Feel free to note the assumptions, skip the mathematics, and read ahead to see if the conclusions look compelling.* Those who want more mathematical background in dynamical systems, the area of mathematics relevant to the models, can turn to a series by Abraham and Shaw (1983) called *Dynamics—the Geometry of Behavior.* These books are profusely illustrated, entertaining, and assume only basic calculus.

By a system of coupled oscillators we shall mean a number of individual oscillating units, each of which is able to oscillate stably on its own when uncoupled from the others, but all of which can affect each other's behavior due to coupling. The effect of one oscillator on another may be direct, as in the case of two neighboring oscillators in a system with nearest neighbor interactions (see Fig. 1), or it may be indirect, as in the case of two distantly separated oscillators in the same system. Note that the interaction between two oscillators may be one-way, as in studies of biological clocks forced by the daily solar cycle (in which case the sun is seen as an oscillator which forces the biological system, but is unaffected itself by the interaction), or the interaction may involve two-way coupling, in which case both oscillators influence each other's behavior (Fig. 2). This formulation is similar to that proposed for the vertebrate locomotor CPG by Grillner (1981) and by Cohen and Wallén (1980).

2 BIOLOGICAL OSCILLATORS

By a biological oscillator we shall mean a biological system which may be modeled by a *structurally stable* dynamical system which exhibits a unique and *asymptotically stable limit cycle.* Structural stability means that the system continues to behave in a qualitatively consistent fashion, *no matter how it is changed,* assuming only that the changes are sufficiently small. Such mathematical changes (called "perturbations") could represent physical changes made by the experimenter, such as dissection of the organism to study the system more easily. Alternatively, they could be due to sensory input arising naturally or artificially, or they could be due to input from

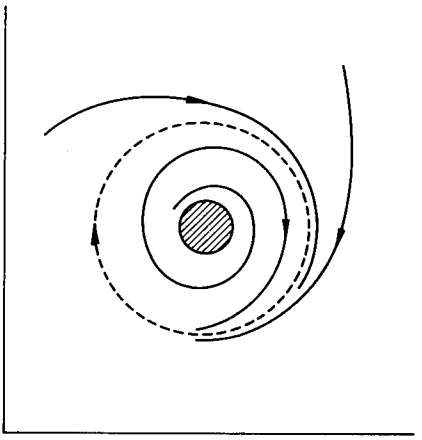

FIGURE 3. Limit cycle oscillator in a two dimensional state space. Shaded region shows quiescent states which do not lie in the basin of attraction of the limit cycle (the dashed trajectory).

other oscillators to which the oscillator in question is coupled. In any case, we assume that the individual unit can oscillate both when it is alone (uncoupled) as well as when it is in the system. That is, we assume that it exhibits stable periodic behavior (called a "limit cycle") which represents the long-time behavior of almost every motion of the system, independent of its initial state. The "basin of attraction" of a limit cycle is all those initial conditions which lead the system to eventually approach that limit cycle. We note that there may be some initial conditions such as extreme temperature and anoxia from which the system cannot attain stable behavior because the conditions do not lie in the basin of attraction of the limit cycle, but we shall ignore the possibility that the oscillator reaches such states (Fig. 3). In other models of excitable membranes the possibility of conditional oscillation or bistable membrane behavior (i.e., either oscillatory or quiescent, depending upon initial conditions or parameters), may be important, but we do not consider such models here. See Harris-Warrick (Chap. 8) and Kopell (Chap. 10) for further discussion of these concepts.

We make no assumptions about the nature of the "state space" which contains the dynamics of the individual oscillator. The state space should be thought of as a space with axes taken as relevant quantities, possibly measurable, such as ionic concentrations, membrane potentials, ionic currents, displacements, velocities, and so on. Thus, a point in the state space represents a particular set of values for the variables being measured (i.e., a "state") and a path parametrized by time in the state space represents the evolving states of the system. We do not claim that the state variables represent any particular specified quantities, although in a specific example one may apply the general theory to a definite state space. In prac-

tice, such a model is highly general, requiring knowledge only of the phenomenologically observed oscillations of the system. The mechanisms giving rise to the oscillations need not be understood. Such a model makes no attempt to model the structure of the oscillator itself and will not be useful for studying the origin of the oscillation, but is quite useful for studying the collective behavior of a system of oscillators whose underlying neuronal structure is unknown.

We now consider the mathematical representation of a single uncoupled biological oscillator. We shall distinguish between the following two effects for motions which start inside the basin of attraction of the stable limit cycle: first, there is the fairly rapid attraction onto the limit cycle, and, second, there is the oscillatory motion around the limit cycle. The first effect possibly corresponds to start-up, for example, as the elements of the oscillators are excited above threshold. This phase is transient and, in many biological systems, disappears after one or two cycles (Pavlidis, 1973, Winfree, 1980). In view of the transient nature of this effect, and in order to obtain a simpler mathematical model, we shall neglect the transient approach to the limit cycle and shall, rather, assume that the oscillator is on its steady state limit cycle at all times. This permits us to specify the state of a single oscillator by a single variable $\theta(t)$, where $\theta(t)$ represents the position of the oscillator *around* its limit cycle at time t, i.e., $\theta(t)$ is the *phase* of the limit cycle (see Fig. 4). Thus the phase of the oscillator is a single variable which realistically reflects the behavior of the most important variables which underlie the oscillation. While this is a dramatic simplification, it seems to be legitimate biologically. We shall rescale θ so that it goes from 0 to 2π radians (= 360 degrees) over one cycle, and we shall parametrize θ so that it flows uniformly around the limit cycle. That is, θ is proportional to the fraction of the period which has elapsed. In applying this model to experimental situations, we will ignore the fine structure of the cycle and look only at some well defined event such as the onset of the

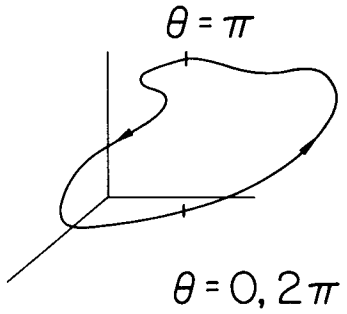

FIGURE 4. The state of a limit cycle oscillator in an n-dimensional state space is represented by the single variable $\theta(t)$, its phase, chosen to run from 0 to 2π around one cycle, and computed mod 2π.

burst. The comparable point will be used in all cycles to delineate $\theta = 0$. This yields the following simple differential equation characterizing a single oscillator:

$$\frac{d\theta}{dt} = \omega \tag{1}$$

where ω is the frequency of the oscillator and $2\pi/\omega$ its period. The solution of this equation is:

$$\theta(t) = \omega t + \theta(0) \tag{2}$$

where $\theta(0)$ is the initial value (at time $t = 0$) of θ.

Although this equation predicts that (t) is an ever increasing function of t, we shall interpret θ to always lie between 0 and 2π. Since motion around the limit cycle is topologically circular, we do not distinguish between one oscillation and the next, but rather start measuring θ anew each time θ crosses 2π. This is accomplished mathematically by using modular arithmetic: Given a value of θ, we add or subtract multiples of 2π to it until the result lies in the interval $0 \leq \theta < 2\pi$. In this case eq. (2) is written:

$$\theta(t) = \omega t + \theta(0) \pmod{2\pi} \tag{2}$$

Geometrically this means that θ is pictured as a point moving on a topological circle rather than on a straight line.

Note that in terms of a state variable $x(t)$ (an axis of the state space), the motion of the oscillator around its limit cycle is given by its projection onto the x-axis. The model offers no prediction as to the wave shape of the resulting periodic function, except that its period must be $2\pi/\omega$ (see Fig. 5). This apparently serious shortcoming of the model is the price we pay for tractability of the ensuing equations. Mathematically speaking, we cannot distinguish between almost sinusoidal (weak) limit cycles and relaxation oscillations (cf. Kopell, Chapt. 10). In short, we have eliminated all references to wave shape except for the phase $\theta(t)$. To account for the observed ventral root output of the lamprey cord, one imagines that a threshold effect causes the spiking process to occur only for a definite range of values of the phase $\theta(t)$, see Figure 5.

For several applications where the oscillator is known purely phenomenologically, this treatment is particularly suitable, in spite of its limitations. In such systems the only measurable variable may be the presence or absence of nerve or muscle activity, or membrane polarization of passively driven output elements, the details of the internal variables being essentially unknown. Thus, one could model the CPG for mastication beginning with the assumption that the CPG is composed of a group of coupled oscillators, each of which controls the activity of one muscle or

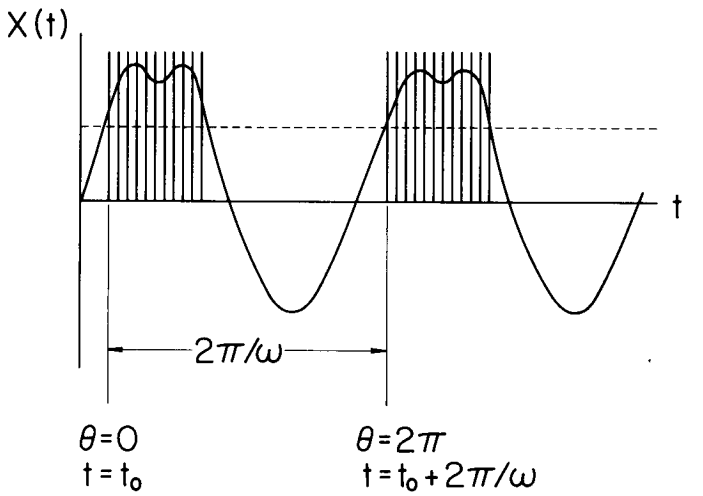

FIGURE 5. Relationship between $\theta(t)$ and $x(t)$ in a limit cycle oscillator which spikes when $x(t)$ is larger than some threshold value (shown dashed).

group of synergistic muscles. In such a model, one could simply use the onset of muscle activity in the various muscle groups to denote $\theta = 0$ for each oscillator. Similarly, in cat locomotion one could make the same set of assumptions with $\theta = 0$ as the onset of activity in the limb muscles. This approach permits us to test assertions regarding the coordinating system while knowing little about the oscillator *per se*, and is in contrast to work in which fairly detailed models of specific physiological processes are developed (e.g., Rinzel, to appear; Chay and Rinzel, to appear).

3 COUPLED OSCILLATORS

Since one of our goals is to develop a method rather than a specific model, we have chosen to use the simplest formulations for our equations. We constructed the oscillators of our models to be non-linear and stable but easily dealt with analytically. Particular assumptions can be added or changed to make them more like a given system or to test a specific hypothesis regarding some component of the system. Such a change will alter the behavior of the system in ways that must be determined for each case. The coupling we have chosen is also characterized by its simplicity, rather than its reality. Again, it can be changed in each case as information is obtained, and again, the behavior of the system in each case must be redetermined. As the discussion progresses we will compare the assumptions used here to those of Kopell. We will also point out the effect the differences have on the conclusions we derive. Essentially, Kopell has gen-

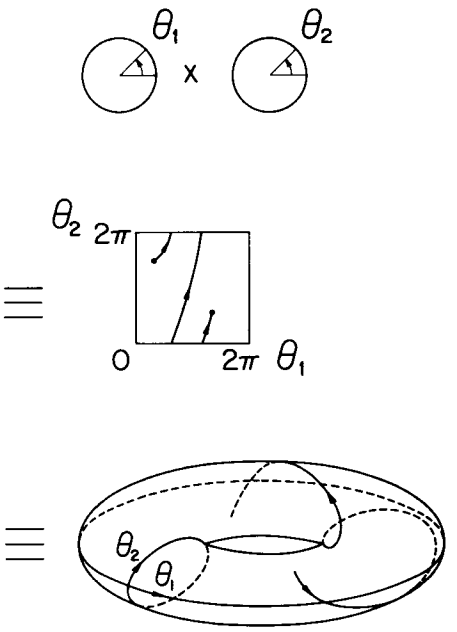

FIGURE 6. Two oscillators are viewed as living on a torus instead of on their individual circles.

eralized the basic formulation set forth in Cohen et. al. (1982) and summarized here. She has also included refinements which make the model conform more to the biology. Some people may find it helpful to start with our formulation which, although unrealistically simplified, is designed to be a skeleton upon which assumptions can be hung and within which changes can be made. Further discussion of the differences between the two approaches will be presented as relevant now and in Kopell's chapter (Chapt. 10).

Let us consider a system of N coupled biological oscillators, each modeled in the manner just described. Corresponding to the ith oscillator (where i is an integer between 1 and N) there will be a phase $\theta_i(t)$ which describes its state at time t. Each phase θ_i will be viewed as living on a circle, $0 \leq \theta_i < 2\pi$. Hence the entire system of N oscillators will live on N such circles. Rather than think in terms of N circles, we will use the usual mathematical convention of "multiplying" these together to give an N dimensional torus T^N. (For example, in the case of $N = 2$ oscillators, we may picture the relationship between the two circles and the 2 dimensional torus T^2 via the intermediate step of identifying the sides of a square in the $\theta_1 - \theta_2$ plane. See Fig. 6.) Thus a vector $\bar{\theta} = (\theta_1, \theta_2, \ldots, \theta_i, \ldots, \theta_N)$ specifies a point on T^N; the N components of the vector tells us where we are relative to each independent circular coordinate.

Here we assume that the limit cycles which characterize the dynamics of the individual oscillators continue to exist after the oscillators are coupled together. Although the shape of the individual limit cycles may change as the nature of the coupling changes, our scheme for parametrizing the θ_i's to run from 0 to 2π around a cycle always permits us to refer to the same N-torus T^N to describe the motion of the system. Our assumption of the structural stability of the individual oscillators implies that, for sufficiently weak coupling relative to the individual oscillator's transient dynamics, the system of coupled oscillators will continue to oscillate stably.

We may obtain a mathematical representation of the system of N oscillators by including coupling terms in eq. (1) written for the ith oscillator:

$$\frac{d\theta_i}{dt} = \omega_i + h_i(\theta_1, \theta_2, \ldots, \theta_N) \tag{3}$$

in which ω_i is the (uncoupled) frequency of the ith oscillator, and the function h_i represents the direct effects of coupling by other oscillators on the ith oscillator. The frequencies ω_i of the individual oscillators may or may not be equal. In the lamprey, for example, the frequencies of the oscillators in a given cord have been found to be equal in some cases, but generally are not (Fig. 7; Cohen, 1984). There will be more detailed discussion of the effect of the ω_i parameters in later sections of this paper.

If the oscillator is more complex, some more complicated function could be added to this equation. For example, if one were modeling the interaction between the cerebellum and the locomotor CPG of cats, one would first note that the cells of the dorsal spinocerebellar tract (DSCT) were not themselves oscillatory but are rhythmically driven by input from the CPG (cf. Gelfand et al., this volume). To model such a neuron one might choose a function $f(\theta)$ with zeroes (points θ^* at which $f(\theta^*) = 0$) so that the equation for the cell $\theta_k' = f(\theta_k)$ sits at a constant phase when isolated. Addition of couplings $h_k(\theta_1, \ldots, \theta_N)$ can then set it in oscillatory motion at the same frequency as the CPG. Such a cell also receives influences from other neurons in the brain and sensory inputs ascending from the limbs and so its equation should include a term which incorporates the influences from these other structures.

Since in our basic model the ith oscillator is described by reference only to its phase θ_i, the coupling function h_i also depends only on the θ_i's (and not, for example, on the size of the limit cycle, or any other characteristics of its wave shape.) The coupling function h_i we must choose to be 2π-periodic in each of its arguments, in order that the "flow" (3) be uniquely defined on the torus T^N. That is, the rate of change of θ_i is to depend only upon the position of each of the N oscillators in their cycles, and not upon how many cycles have already passed (cf. the modular arithmetic discussion above.)

We further assume that the coupling may be separated into contribu-

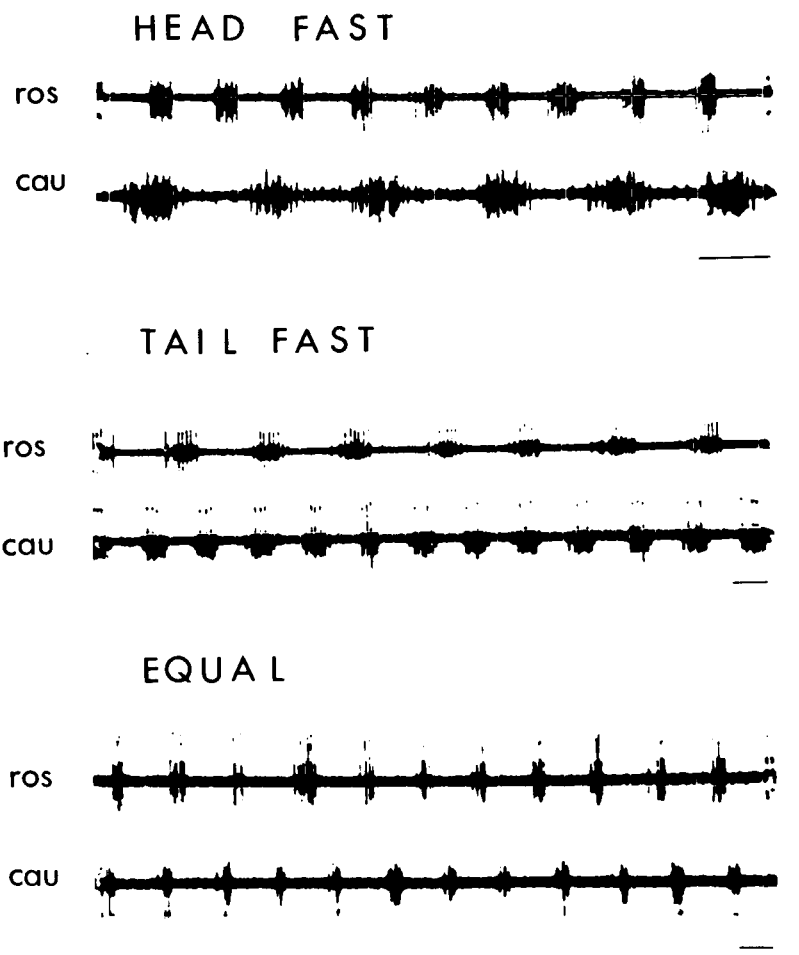

FIGURE 7. Ventral root bursting of separated rostral and caudal pieces of isolated lamprey spinal cords. Prior to cutting, the cords all generated well-coordinated traveling waves when stimulated with D-glutamate. The cords, all treated alike, were cut through at their mid-segments, kept under the same conditions and recordings continued. These traces were photographed after the drug was removed and reapplied to allow damaged fibers to quiet down.

tions due to the interaction between any two pairs of oscillators. In each part of the equation one oscillator is presynaptic and the other postsynaptic. Mathematically this means that we may write the coupling function h_i as the sum of a series of N terms:

$$h_i(\theta_1, \theta_2, \ldots, \theta_N) = \sum_{j=1}^{N} h_{ij}(\theta_i, \theta_j) \tag{4}$$

where the function h_{ij} represents the effect of the jth oscillator on the ith oscillator (and hence depends only on θ_i and θ_j). The jth oscillator is, therefore, presynaptic to the ith oscillator in (4), and h is assumed to be 2π-periodic in its arguments.

How shall we specify the coupling functions h_{ij} ? To begin with, we will require that h_{ij} be zero when both oscillators are at the same points in their cycles, i.e., when θ_i equals θ_j. This assumption will, as we shall see, permit two identical coupled oscillators to oscillate in phase with each other, as intuition requires. (See Kopell, Chapt. 10, for an alternative form of coupling she terms "synaptic coupling.") Mathematically, this can be accomplished by requiring that h_{ij} depend only on the difference between θ_i and θ_j:

$$h_{ij}(\theta_i,\theta_j) = h_{ij}(\theta_j - \theta_i) \tag{5}$$

such that $h_{ij}(0) = 0$. Such coupling is called diffusive coupling. In Kopell's formulation, h_{ij} also depends on $(\theta_j - \theta_i)$ but need not be zero when $\theta_j - \theta_i = 0$. (Cf. Kopell for further discussion of the significance of this assumption.) Now since the function h_{ij} must be 2π-periodic, we can develop it in a Fourier series of sines and cosines. Taking just the first terms of the Fourier series, we obtain:

$$h_{ij}(\theta_i, \theta_j) = a \sin(\theta_j - \theta_i) + b[1 - \cos(\theta_j - \theta_i)] \tag{6}$$

where a and b are coupling coefficients. We shall take $b = 0$ in what follows (after Cohen et al., 1982), thus making h the pure sine function, but we note that Ermentrout and Kopell (1984) have discussed the effects of including the cosine terms. The latter play an important role in some situations especially with respect to the resultant frequency of the system and to the uniformity of the phase lags in a chain of many oscillators. A coupling function of the form (6) was derived by an independent approach (a perturbation method) in the case of two weakly coupled van der Pol oscillators (Rand & Holmes, 1980), and in more general situations by Neu (1979, 1980).

Substituting (4) – (6) into (3) we obtain:

$$\frac{d\theta_i}{dt} = \omega_i + \sum_{j=1}^{N} a_{ij} \sin(\theta_j - \theta_i) \tag{7}$$

where a_{ij} is the coupling coefficient representing the influence of oscillator j on oscillator i. a_{ij} is assumed to be independent of the oscillator, undoubtedly an incorrect assumption. However, superficial attempts to change this have not yielded anything very interesting to date, but more needs to be done to explore fully this level of complexity. Note that *positive* values of a_{ij}

tend to advance the phase of θ_i, if θ_j leads θ_i by a small amount, and hence are called *excitatory.* Similarly, *negative* a_{ij} are called *inhibitory* (cf. Kopell, Chapt. 10 in which the terms "desynchronizing" and "synchronizing" are used instead).

These differential equations (7) are nonlinear and no exact general solution can be expected to be found for arbitrary parameter values. Nevertheless, it is possible to learn much about the behavior of these equations by (1) looking for exact special solutions and (2) numerically integrating them on a digital computer.

In the rest of this chapter, we shall consider various special cases of eqs. (7) and associated applications, as well as extensions of the model to more complicated coupling functions.

4 TWO COUPLED OSCILLATORS

Many biological systems can be modeled as consisting of two coupled oscillators. For example, the CPGs for each limb of a quadruped can be modeled as a chain of several oscillators (cf. Grillner, 1981; Cohen, Chapt. 5). However in dealing with the coordination between the two limbs of a single girdle, they can more conveniently be viewed as a pair of coupled oscillators where the oscillators for the various muscle groups are lumped together and taken as a single limb oscillator. Moreover, the following simple systems serve as a good introduction to help understand the behaviors exhibited by larger collections of oscillators. In the case of two oscillators, eqs. (7) become:

$$\frac{d\theta_1}{dt} = \omega_1 + a_{12} \sin(\theta_2 - \theta_1) \tag{8a}$$

$$\frac{d\theta_2}{dt} = \omega_2 + a_{21} \sin(\theta_1 - \theta_2) \tag{8b}$$

It is convenient to define a quantity

$$\varphi(t) = \theta_1(t) - \theta_2(t) \tag{9}$$

which represents the phase lag of oscillator 2 relative to oscillator 1. Like θ_1 and θ_2, φ lives on a circle. The phase lag φ satisfies a relatively simple differential equation which is obtained by subtracting (8b) from (8a), giving:

$$\frac{d\varphi}{dt} = (\omega_1 - \omega_2) - (a_{12} + a_{21}) \sin \varphi \tag{10}$$

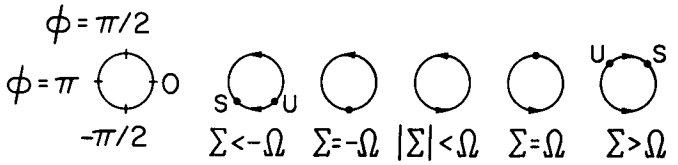

FIGURE 8. Bifurcation of equilibrium states of eq. (10) (representing phase-locked motions). In this sequence of flows on the φ circle, we assume that $\omega_1 > \omega_2$ (and set $\Omega = \omega_1 - \omega_2 > 0$). We let $\Sigma = a_{12} + a_{21}$ vary from $-\infty$ to $+\infty$. The positions of the equilibria are given by dots, the location of which are found from eq. (11). As indicated by the directions of the arrows, the stable equilibria are marked S, and the unstable U. For $0 < \Omega < \Sigma$ (excitatory coupling), the stable equilibrium point satisfies $0 < \varphi < \pi/2$ and oscillator 1 (the faster of the two) leads oscillator 2. For $\Sigma < -\Omega < 0$ (inhibitory coupling), on other hand, the stable equilibrium satisfies $-\pi < \varphi < -\pi/2$ and the slower oscillator (oscillator 2) leads.

This single differential equation can be solved exactly (see Cohen et al., 1982). It is sufficient for us here, however, to look for special solutions, called 1:1 phase-locked motions, in which the phase lag $\varphi(t)$ is a constant over time. These motions are represented by the equilibria of (10), and may be obtained by equating the right-hand side of (10) to zero:

$$\varphi = \arcsin \frac{\omega_1 - \omega_2}{a_{12} + a_{21}} \tag{11}$$

Eq. (11) has either 0, 1, or 2 solutions, depending upon whether the key quantity, the ratio of frequency difference to coupling.

$$\left| \frac{\omega_1 - \omega_2}{a_{12} + a_{21}} \right| \tag{12}$$

is greater than, equal to, or less than unity. (Since the sine function always has absolute value less than or equal to unity, there will be no solutions if (12) is greater than 1. Note that this result depends on the form assumed for the coupling function h (eqs. (6), (7).) If a different function h were chosen, a similar analysis would be required and the results may or may not support phase-locked motions (see Fig. 8). In the case that no such phase-locked solutions occur, the system is said to drift. The same qualitative bifurcation into drift will hold for any bounded 2π periodic function, although more than one stable solution might exist in the locked region.

In words, this result states that phase (and frequency) locking will occur if the difference between the frequencies of the two oscillators is sufficiently small, compared to the net coupling between them. For two given oscillators (with their frequencies ω_1 and ω_2 fixed), the coupling may be increased until a critical value is reached at which point the system goes from drift to phase-locked motion. As we will see later, in the transitions

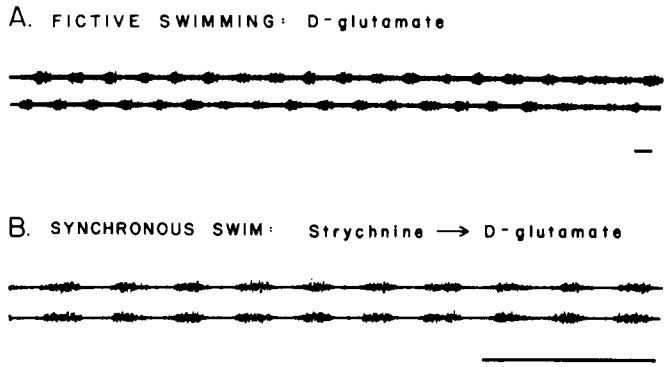

FIGURE 9. Strychnine-induced synchronous bursting. The recordings are from the left and right roots of a single segment. Top traces: before strychnine with D-glutamate alone. Lower traces: after strychnine was applied to cord, removed and D-glutamate readded. (Adapted from Cohen & Harris-Warrick, 1984. See reference for details). Time bar = 1 second.

there may be what has been termed "relative coordination" (von Holst, 1939, transl. 1973), as has been observed in fish by von Holst (1939, transl. 1973) and in lamprey by Cohen (Cohen et al., 1982; Cohen, 1984). From eq. (11) it follows that once locking has occurred, if the net coupling is positive (excitatory), then the faster oscillator will lead by a phase angle between 0 and 90 degrees, while if the net coupling is negative (inhibitory), then the slower oscillator will lead by a phase angle between 90 and 180 degrees. These last conclusions follow from consideration of the stability of the phase-locked states, and can be seen from the direction of the arrows generating the flow on the φ circle in Figure 8. It is interesting to observe that in a simple, two-oscillator system, this could afford a mechanism for reversing the direction of motion, say, from forwards to backwards, simply by changing the relative frequencies of the oscillators.

As an example of an application of this model to a biological problem in which the two oscillators have similar frequencies, we consider an experiment by Cohen and Harris-Warrick (1984) involving the treatment of the isolated lamprey spinal cord with strychnine. Briefly, we postulate that each segment, or small group of segments of the cord contains two oscillators which normally burst about 180 degrees (π radians) out-of-phase. In the in vitro preparation, this is called "fictive swimming" (cf. Grillner et al., Chapt. 1 and Cohen, Chapt. 5). After pre-treatment with strychnine, the two sides are observed to oscillate approximately in phase, with roughly synchronous bursting (Fig. 9). Although the details of the effect of strychnine are not completely known, it is known that in the lamprey spinal cord strychnine blocks inhibitory glycinergic synapses (Homma and Rovainen, 1978).

In order to explain this behavior with the foregoing model, we assume

that the left and right sides of the cord can be "lumped" into two oscillators with approximately the same uncoupled frequencies ($\omega_1 \approx \omega_2$). The oscillators along the entire cord almost certainly do not have the same frequencies but the two within each segment almost certainly do have very close frequencies. Thus, $\omega_1 - \omega_2 \approx 0$. Since the normal functioning of the cord displays phase-locked alternation with $\varphi = \pi$, we assume that the net coupling is initially inhibitory ($a_{12} + a_{21} < 0$). The addition of strychnine is then modeled as removing the inhibitory coupling, leaving a net excitatory coupling ($a_{12} + a_{21} > 0$). This moves the dynamical state from the initial state out-of-phase equilibrium $\varphi \approx \pi$ to a new in-phase equilibrium given by $\varphi \approx 0$. Moreover, the model predicts that as the strychnine gradually takes effect, the net coupling must pass through zero (since it goes from net negative to net positive). For some range of coupling values around zero (depending on the frequency difference $\omega_1 - \omega_2$) no phase-locked states exist (cf. eq. (11)), and the model predicts a temporary period of drift. The model system, although it must drift for a time, can move continuously through the transition from alternation to synchrony. However, in the experimental system, the situation is more complex. The cord is unable to pass into and out of the period of drift. Adding strychnine directly to a fictively swimming preparation causes the cord to burst unstably and, finally, tonically, with all evidence of oscillation gone. The only method of application that produces stable bursting is to remove the glutamate from the bath, perfuse the cord with strychnine for some time, and immediately add the glutamate after removing the strychnine (which remains bound to the receptors for well over half an hour). The supposition is that this difference between the model and the cord will be reflected in the imbedding of the two oscillators in their respective multidimensional phase spaces, an aspect which our simple phase model cannot address and which we have so far ignored.

This simple formulation of the model can also be applied to experiments by Young et al. (1980) on the *scaphognathite* of the lobster, *Homarus americanus*, and by Kammer on several species of Lepidoptera (1968). In the experiments of Young et al., picrotoxin, which blocks inhibitory synapses, was able to induce changes in the ventilatory motor output pattern very similar to those predicted in the discussion above. The bursting was transformed by picrotoxin from an out-of-phase mode, through a long period of instability and drift, to a stable in-phase mode (Fig. 10). Kammer recorded motor activity during the change from warm-up to flight in several species of moths. She obtained a variety of "shivering" patterns, but a relatively common observation was that muscles would fairly rapidly switch from the synchrony of shivering to the alternation needed for flight. This would suggest a mechanism similar to that proposed above, but with the switch being from excitatory to inhibitory coupling. Kammer proposed a model qualitatively similar to ours in order to explain her findings.

The transition from trot to gallop in tetrapods may also have some of

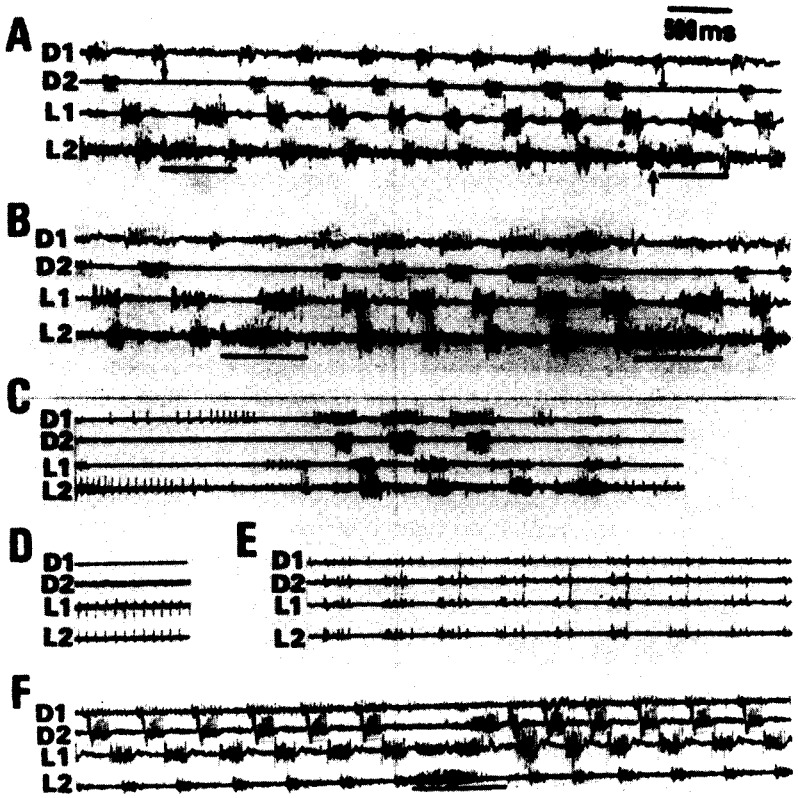

FIGURE 10. Effect of picrotoxin (ptx) on phasing of the scaphognathite muscles during rhythmic activity. (A) Activity before ptx treatment. Bursts underscored are reversals, arrows indicate changes in pattern associated with the reversal. Notice the minimum overlap between D1 and D2. (B) Activity 6 minutes after treatment with the ptx. Notice the phasing has changed with D1 and D2 now overlapping considerably. L and D groups still alternate (C) Activity 9 minutes after treatment. Brief periods of rhythmic pumping interrupt periods of long, overlapping though still weakly reciprocating bursts of increasing length. By 10 minutes no rhythmic activity was seen. (D) BY 15 minutes L1 started firing and the two L group muscles showed tonic, synchronous activity for about 15 minutes. (E) By 65 minutes tonic synchronous spikes and bursts appeared in all groups. (F) By 90 minutes normal rhythmic activity returned. (Adapted from Young et al., 1980. See reference for more details.)

the model's features. In cats, each limb continues to oscillate normally as the animal changes from trot to other fast gaits, such as canter and gallop. However, English has noted (1979) that the limbs pass through highly variable phase relations as they change from the slower alternating to the faster non-alternating gaits. One interpretation for the variability is that drift occurs between limb oscillators as the coupling between the limbs changes from inhibitory to excitatory coupling.

As a different type of example of the two-oscillator model, we consider

the experiments of Cohen concerning the surgical lesioning of the isolated lamprey cord. Briefly, the experiment consists of making a specific lesion in the cord and observing the changes in dynamics of bursting. It is found that the groups of segments rostral and caudal to the lesion remain internally phase-locked, but the two groups can be seen to drift with respect to one another. The extent and nature of the drift is dependent on the kind of lesion. The drift state can be characterized by plotting "period" of oscillation (i.e., time between consecutive appearances of the same phase in the cycle, in this case the onset of the bursting) as a function of time (see Fig. 11).

This situation has been modeled (Cohen et al., 1982) by taking the rostral and caudal groups of segments on either side of the lesion as individual oscillators. We assume, in accord with the more common experimental observation, that the frequencies of the oscillators differ (Cohen, 1984). In order to compare the model with the experiment, we graph the behavior of the model oscillators as described above. The period of time between consecutive zero phases is plotted against time for both oscillator 1 and oscillator 2 (see Fig. 12). Note that in the extreme case of one-way descending coupling, where the lesion has destroyed all the ascending coupling, the forcing oscillator is perfectly stable while the forced oscillator shows great instability. Comparison of Figures 11 and 12 led to the conjecture that, in the experimental cord, the spared medial tracts contain fibers which primarily descend from head to tail. Similar types of evidence suggest that the lateral tracts contain both descending and ascending fibers (Cohen, 1986; Rovainen, 1985). More experimental work is needed to confirm these conjectures, but they remain as working hypotheses.

It is important to note that with h, the coupling, as the sine function, the frequency of the pair of coupled oscillators will be intermediate between the frequencies of the uncoupled pair. However, with couplings other than the sine function, the frequency of the coupled system will still depend on ω_1, ω_2 and h, but it need not be intermediate between ω_1 and ω_2 (cf. Kopell, Chapt. 10).

5 CHAIN OF N OSCILLATORS WITH NEAREST NEIGHBOR COUPLING

We return now to consideration of eqs. (7) in the general case of N coupled oscillators. We start by considering a chain of N oscillators with nearest neighbor coupling (Fig. 1), a configuration which is certainly oversimplified, but which is useful in beginning to model the lamprey CPG (Cohen et al., 1982). It also applies to waves in the mammalian intestine (Ermentrout and Kopell, 1984), and stomatal oscillations in the leaves of green plants (Rand et al., 1982). In this case, eqs. (7) become:

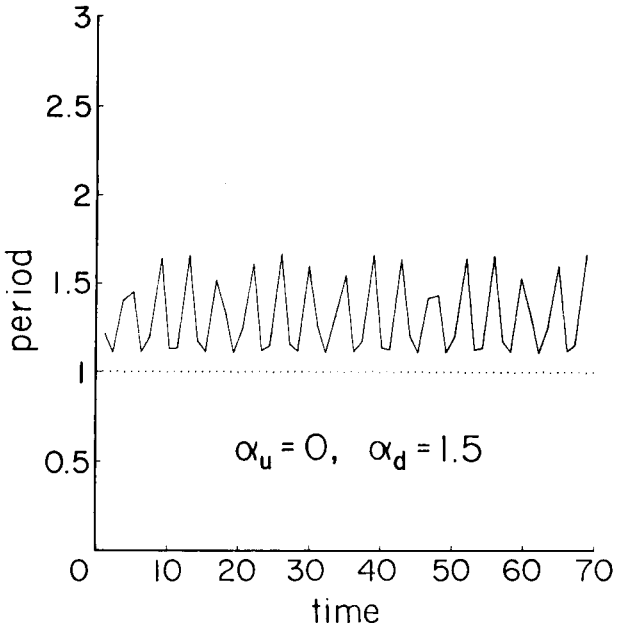

FIGURE 11. Upper figure. Graph of period versus time for two model oscillators. The dotted line is the "rostral" and the solid, the "caudal". We assume the ascending coupling (α_u) has been lesioned leaving only the descending ocupling (α_d) reduced but still present. When uncoupled period of "rostral" is 1 and "caudal" is 1.5. (From Cohen et al., 1982.)

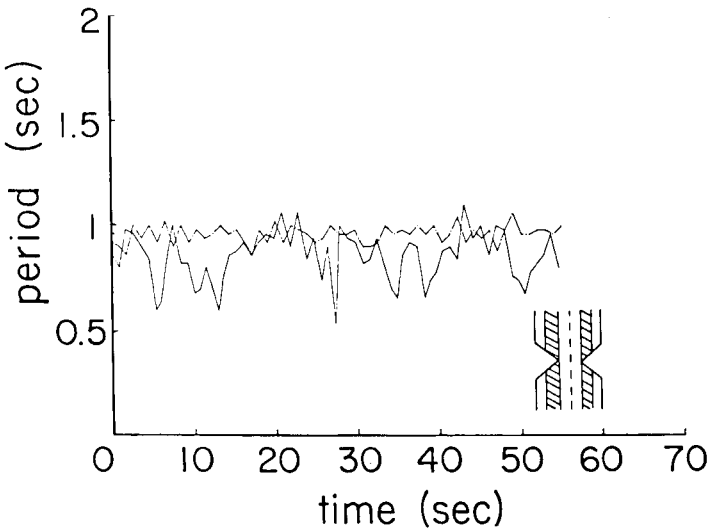

FIGURE 12. Lower figure. Period of successive bursts versus time for two ventral roots of a lesioned lamprey spinal cord (see insert) Rostral root is dotted, caudal is solid. Caudal is considerably more variable than rostral with pattern of variability similar to that of theoretical oscillators in Fig. 11. (From Cohen et al., 1982.)

$$\begin{aligned}
\frac{d\theta_1}{dt} &= \omega_1 + a \sin(\theta_2 - \theta_1) \\
\frac{d\theta_i}{dt} &= \omega_i + a \sin(\theta_{i+1} - \theta_i) + a \sin(\theta_{i-1} - \theta_i) \\
\frac{d\theta_N}{dt} &= \omega_N + a \sin(\theta_{N-1} - \theta_N)
\end{aligned} \tag{13}$$

where $i = 1,2, \ldots, N$ and where we have assumed for convenience that all the coupling constants are equal, $a_{ij} = a$.

Following the treatment of the two oscillator case, we set $\varphi_i = \theta_i - \theta_{i+1}$ for $i = 1,2, \ldots, N-1$, cf. eq. (9). From eqs. (13) we obtain the following $N - 1$ eqs. on the ϕ_i, which we write in matrix form:

$$\frac{d\bar{\varphi}}{dt} = \bar{\Omega} + \bar{A}\bar{S} \tag{14}$$

where

$$\bar{\varphi} = \begin{bmatrix} \varphi_1 \\ \ldots \\ \varphi_{N-1} \end{bmatrix}, \bar{S} = \begin{bmatrix} \sin \varphi_1 \\ \ldots \\ \sin \varphi_{N-1} \end{bmatrix}, \bar{\Omega} = \begin{bmatrix} \omega_1 - \omega_2 \\ \ldots \\ \omega_{N-1} - \omega_N \end{bmatrix}$$

are $N-1$ vectors and where

$$\bar{A} = a \begin{bmatrix} -2 & 1 & & \\ 1 & -2 & 1 & \\ & 1 & -2 & 1 \\ & & 1 & -2 \end{bmatrix}$$

is a tri-diagonal $N-1 \times N-1$ matrix representing the coupling constants between all N oscillators.

As in the two oscillator case, we investigate the existence of 1:1 phase locked motions by requiring the φ_i to be constants in (14), giving $d\bar{\varphi}/dt = \bar{0}$ and:

$$\bar{S} = -\bar{A}^{-1}\bar{\Omega} \tag{15}$$

No solution of (15) exists if any of the components of $\bar{A}^{-1}\bar{\Omega}$ are larger than unity in absolute value (since each of the components of $\bar{S}$ are sines).

Now it turns out (Cohen et al., 1982) that the matrix $\bar{A}$, although arbitrarily large, is tractable, since it can be inverted in closed form. For example, in the case of $N = 6$ oscillators, $\bar{A}$ is a 5×5 matrix with inverse:

$$\bar{A}^{-1} = -\frac{1}{6a}\begin{bmatrix} 5 & 4 & 3 & 2 & 1 \\ 4 & 8 & 6 & 4 & 2 \\ 3 & 6 & 9 & 6 & 3 \\ 2 & 4 & 6 & 8 & 4 \\ 1 & 2 & 3 & 4 & 5 \end{bmatrix} \tag{16}$$

Thus, we can compute the phase lag vector $\bar{\varphi}$ in closed form.

As an example, suppose that the difference in frequencies, ω_i along the chain is a constant, i.e., $\omega_1 - \omega_2 = \omega_2 - \omega_3 = \ldots = e$. Then

$$\bar{\Omega} = e\begin{bmatrix} 1 \\ 1 \\ \cdots \\ 1 \end{bmatrix} \tag{17}$$

and in the case of $N = 6$ oscillators, eq. (15) becomes (using (16)):

$$\begin{bmatrix} \sin\varphi_1 \\ \sin\varphi_2 \\ \sin\varphi_3 \\ \sin\varphi_4 \\ \sin\varphi_5 \end{bmatrix} = \frac{e}{2a}\begin{bmatrix} 5 \\ 8 \\ 9 \\ 8 \\ 5 \end{bmatrix} \tag{18}$$

Note that the condition on φ_3 is the hardest to satisfy, and phase-locked solutions exist only if

$$\left\| \frac{e}{a} \right\| \leq \frac{2}{9} \tag{19}$$

For general N, it can be shown that eq. (19) generalizes to $|e/a| \leq 8/N^2$ (N even), or $|e/a| \leq 8/(N^2-1)$ (N odd), and that the resulting motion is frequency-locked at the average frequency of the uncoupled oscillators. For $N = 2$ this gives $|e/a| \leq 2$, which is just expression (12) equated to unity. When $e = 0$, the chain oscillates in unison with $\varphi = 0$, that is, there is no traveling wave.

Returning to the example of N=6 oscillators, Fig. 13 shows the predicted phase lags for $e/a = 0.01$ and 0.22. Since each of the φ_i's is positive, the faster oscillators lead the slower ones in each pair of neighbors (assuming e and a are positive), the greatest phase difference occurring at the middle of the chain, between oscillators 3 and 4. It should be noted that the experimentally measured phase difference between nearby oscillators in the midbody region and at the ends of the cord is actually always quite small. Moreover, no differences in phase lags have so far been observed along the cord, but a small difference could be difficult to measure reliably.

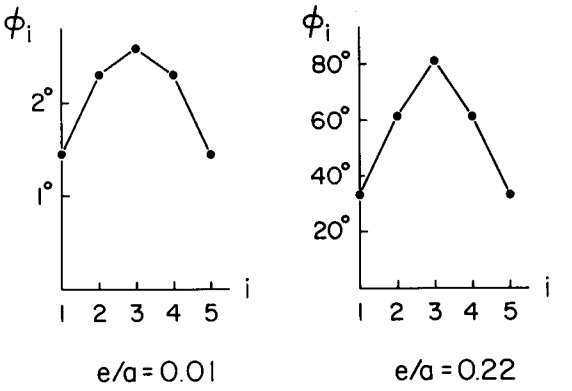

FIGURE 13. Plot of φ_i for a system of 6 oscillators with $\bar{\Omega} = (e, e, e, \ldots, e)$.

Alternatively, this discrepancy could be an indication that the ratio of the frequency difference to coupling constant *e/a* is quite small or that the assumptions of sine coupling and strictly nearest neighbor coupling are inappropriate for the lamprey (cf. Kopell for *h*, not the sine function).

In the case that eq. (19) is not satisfied, the system of $N = 6$ oscillators is not 1:1 phase-locked. Ermentrout and Kopell, (1984) have studied what happens to a chain of N oscillators with nearest neighbor coupling when the parameters are tuned to just outside the point of phase-locking. Their results, interpreted in terms of the $N = 6$ example, show that if *e/a* is just slightly larger than 2/9, oscillators 1, 2, and 3 tend to oscillate as one unit; oscillators 4, 5, and 6 oscillate as another unit; but the two groups drift with respect to one another. Ermentrout and Kopell (1984) have followed earlier authors and called this phenomenon "frequency plateaus," and have identified it with the normal functioning of mammalian intestines. In some situations, several plateaus can appear in a long chain of oscillators. In the formulation of Kopell and Ermentrout (cf. Kopell, chapt. 10) N oscillators, with nearest neighbor coupling, can produce a traveling wave with uniform phase lags along the cord. They assume $e = 0$, i.e., that there are little or no frequency differences among the oscillators and that the coupling is "synaptic" ($h(0) \neq 0$). They can address frequency differences of a significant magnitude if they add multiple neighbor interactions (see Kopell, Chapt. 10).

6 DOUBLE CHAIN MODEL

There is considerable, albeit indirect, evidence that the lamprey CPG is actually composed of a double chain of oscillators (Cohen and Harris-Warrick, 1984; Cohen and Wallén, 1980; Grillner et al., Chapt. 1). This fact

is proven unequivocally in the *Xenopus* tadpole, since each half of a subdivided cord can continue to burst (Kahn and Roberts, 1982). To account for this evidence, in the following equation we extend the previous single chain model to a double chain. By doing this we can also begin to demonstrate how the approach presented in this chapter could be applied to a variety of situations. This extension, for example, brings us closer to the realm of more complex CPGs, such as the mammalian locomotor CPG. In such complex CPGs the brachial and lumbar enlargements control their respective joints and limbs with their respective sets of flexors and extensors (Viala and Vidal, 1979); each limb generator in turn is coupled to each other limb generator. As is reflected in the range of gaits limbed animals display (Gambary an, 1974; Hildebrand, 1976), the potential for controlling the coordination under these conditions is enormous, as is the task of understanding them (cf. Cohen, Chapt. 5).

This model involves $2N$ oscillators with phases θ_i^R and θ_i^L for i from 1 to N (L = left, R = right) see Figure 14. The governing equations become:

$$\frac{d\theta_i^L}{dt} = \omega_i + a\sin(\theta_{i-1}^L - \theta_i^L) + a\sin(\theta_{i+1}^L - \theta_i^L) + k\sin(\theta_{i-1}^R - \theta_i^L) + k\sin(\theta_{i+1}^R - \theta_i^L) + c\sin(\theta_i^R - \theta_i^L) \tag{20}$$

$$\frac{d\theta_i^R}{dt} = \omega_i + a\sin(\theta_{-1}^R - \theta_i^R) + a\sin(\theta_{i+1}^R - \theta_i^R) + k\sin(\theta_{i-1}^L - \theta_i^R) + k\sin(\theta_{i+1}^L - \theta_i^R) + c\sin(\theta_i^L - \theta_i^R) \tag{21}$$

where a, k, and c are coupling constants (see Fig. 14), and where we have assumed that θ_i^L and θ_i^R both have the same uncoupled frequencies ω_i. Note that when k and c are zero, eqs. (20), (21) each reduce to eq. (13) for the single chain model.

We now seek a phase-locked solution for "fictive swimming" by setting:

$$\theta_i^R(t) = \theta_i^L(t) + P, \qquad P = 0 \text{ or } \pi \tag{22}$$

Eq. (22) is based on the experimental observation that the left and right sides of the cord are normally 180 degrees out-of-phase, but, with the addition of strychnine, can be made to oscillate in-phase (cf. the foregoing discussion of the two oscillator model). We also take into account the well-known observation that the locomotor CPGs of mammals permit either alternating (trot) or a range of gaits in which the limbs are more or less in-phase (e.g., gallop, bound, hop) (Gambaryan, 1974). In this latter case we make no assumptions regarding the origin of the coupling. It could be propriospinal neurons, descending controlling neurons, or sensory inputs. Here, rather than fixing coupling and frequency parameter values and seeking a phase locked solution, we specify a desired solution and seek the parameter values which would yield it. This approach yields an

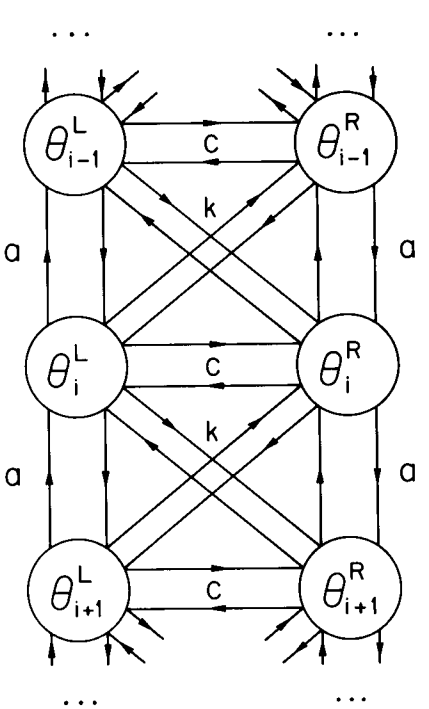

FIGURE 14. Double chain model.

exact solution to the governing equations, but it does not eliminate the possibility that other solutions may exist.

Substitution of (22) into (20), (21) gives:

$$\frac{d\theta_i^L}{dt} = \omega_i + (a \pm k)\left[\sin(\theta_{i-1}^L - \theta_i^L) + \sin(\theta_{i+1}^L - \theta_i^L)\right] \tag{23}$$

where the upper sign corresponds to $P = 0$ and the lower sign corresponds to $P = \pi$, and where, due to (22), we obtain an identical equation on θ_i^R.

Note that the form of eq. (23) is identical to that of the single chain eq. (13), except that the coupling constant a has been replaced by $a \pm k$. (The reason that the single chain model has bearing on the double chain is because we have assumed the special solution (22) in which both sides of the double chain are phase locked together.) In the case that $a = 0$, $k < 0$, and $P = \pi$, the analysis of the single chain model shows that this system exhibits phase-locked motions. This allows us to draw the following important conclusion: The double chain model shows that the lamprey cord can exhibit normal fictive swimming (with left and right sides 180 degrees out-

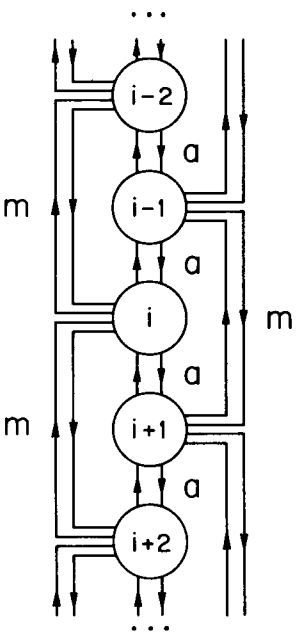

FIGURE 15. A chain of N oscillators with nearest and second nearest neighbor coupling.

of-phase) without excitatory coupling a, but rather with inhibitory coupling k from each oscillator to its upper and lower neighbors on the opposite side of the cord. This fact is particularly interesting in view of results obtained with strychnine. In the lamprey cord, strychnine pretreatment does not block intersegmental coordination, but it does degrade it and change it (Cohen, 1983). This implies that there are both glyceringic fibers (presumably inhibitory) and non-glyceringic fibers (presumably at least partly excitatory), which are components of the intersegmental coordinating system. The model results suggest that the inhibitory fibers may be crossed fibers while the excitatory are uncrossed (see also Rovainen, 1985).

7 CHAIN WITH NEAREST AND SECOND-NEAREST NEIGHBOR COUPLING

Next we shall extend the single chain model (13) to include both nearest and second-nearest neighbor coupling. The lamprey CPG has been shown to have both short and long coordinating fibers (Cohen, 1984). The long fibers can extend over ten or more segments. A model incorporating such a wide range of coordinating fiber lengths would be extremely difficult to deal with mathematically. Second-nearest neighbor coupling is expected to

offer a generalization which, while still far from the actual situation, is a step closer to resembling the features of the cord which we can identify. Referring to Figure 15, the governing equations become:

$$\begin{aligned}\frac{d\theta_i}{dt} = \omega_i &+ a \sin(\theta_{i+1} - \theta_i) \\ &+ a \sin(\theta_{i-1} - \theta_i) + \\ &m \sin(\theta_{i+2} - \theta_i) + m \sin(\theta_{i-2} - \theta_i)\end{aligned} \tag{24}$$

where a and m are coupling coefficients. Once again, defining $\varphi_i = \theta_i - \theta_{i+1}$, we obtain the following matrix equation on the φ_i, expressed in the notation of eq. (14):

$$\frac{d\bar{\varphi}}{dt} = \bar{\Omega} + \bar{A}\bar{S} + \bar{M}\bar{T} \tag{25}$$

where $\bar{\varphi}$, $\bar{\Omega}$, $\bar{A}$, $\bar{S}$ are as in eq. (14), and where $\bar{M}$ is an $N-1 \times N-2$ matrix of next to nearest neighbor coupling coefficients $\bar{T}$ is an $N-2$ vector given by:

$$M = m\begin{bmatrix} -1 & 1 & & & & \\ -1 & -1 & 1 & & & \\ 1 & -1 & -1 & 1 & & \\ & 1 & -1 & -1 & 1 & \\ & & \cdots & & & \\ & & & 1 & -1 & 1 \\ & & & & 1 & -1 \\ & & & & & -1 \end{bmatrix}, \quad T = \begin{bmatrix} \sin(\varphi_1 + \varphi_2) \\ \sin(\varphi_2 + \varphi_3) \\ \cdots \\ \sin(\varphi_{N-3} + \varphi_{N-2}) \\ \sin(\varphi_{N-2} + \varphi_{N-1}) \end{bmatrix}$$

Note that when $m = 0$ eq. (25) reduces to eq. (14) for the chain with nearest neighbor coupling.

We investigated eq. (25) using numerical integration on a digital computer. We chose the parameter values $\bar{\Omega} = \bar{0}$, i.e., $\omega_1 = \omega_2 = \ldots \omega_N$(identical uncoupled oscillators), and $a = 1$, $m = -1$. This models the case in which the nearest neighbor coupling is excitatory, while the second-nearest neighbor coupling is inhibitory. Before discussing the results, we note that in the case $\bar{\Omega} = \bar{0}$, $a = 1$ and $m = 0$ (oscillators with identical frequencies and nearest neighbor coupling only), eq. (14) predicts that the system will be phase-locked with zero phase lag between any two oscillators (cf. eq. (18) with $e = 0$), i.e., there will be only synchronous bursting with no traveling wave.

The addition of inhibitory nearest neighbor coupling produces the results displayed in Figure 16, which is now drastically different. Eq. (25) was numerically integrated until a steady state was reached. The initial

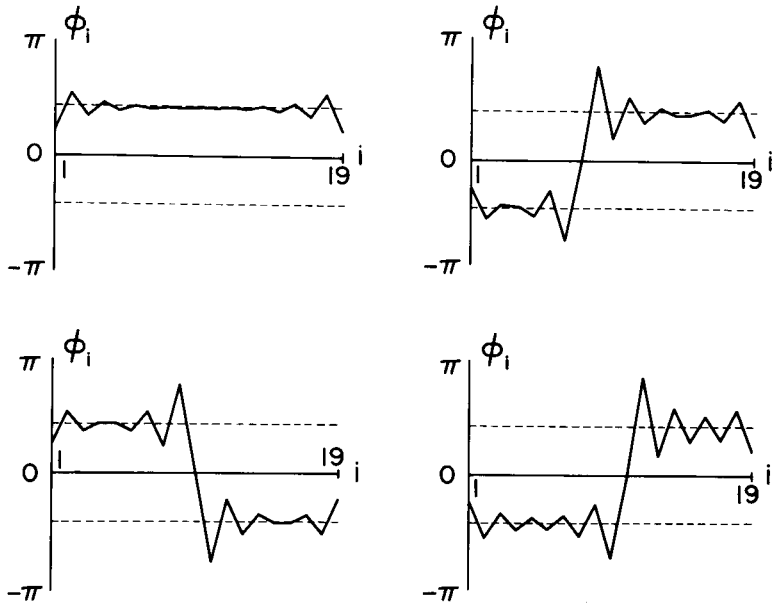

FIGURE 16. Results of numerical integration to a steady state for the system of Fig. 15, eq. (25), for $a = 1$, $m = -1$, $\omega_1 = \omega_2 = \ldots = \omega_{20}$ in the case of N = 20 identical oscillators.

conditions were randomly chosen for the four displayed runs (the coupling and frequency parameters were identical). The great diversity in results means that each of the displayed phase-locked solutions is only locally asymptotically stable, and that the actual state achieved by the system is strongly dependent on the choice of initial conditions. No biological system can afford to operate in this fashion.

Thus, a system of identical oscillators with excitatory nearest neighbor coupling can be destabilized (in the sense of creating an unstable steady state) by adding enough inhibitory second-nearest neighbor coupling. How much inhibitory second-nearest neighbor coupling can be added without destabilizing the zero phase difference state? In order to obtain an analytical answer to this question, we have considered the continuum model in the Appendix.

8 2:1 PHASE-LOCKING

In some cases, after a lamprey cord has been lesioned, the segments above and below the lesion can be phase-locked but with the frequency of those segments on one side of the lesion twice the frequency of those on the other (Fig. 17). Stable 2:1 bursting is rare; it does not occur following any particular lesion or under conditions we can precisely specify. However, a

pattern of two-burst cycles for each movement cycle can be obtained by imposing movement on the caudal end of the cord which is too far outside the preferred frequency of the segmental oscillators (Grillner et al., 1981). 2:1 stepping patterns have also been observed upon occasion in high-spinal turtles (Stein, 1978) and decerebrate chickens (Jacobson and Hollyday, 1982). More stable 2:1 stepping patterns can be induced in decerebrate (Kulagin and Shik, 1970) or chronic spinal kittens (Forssberg, 1980), by placing each of the hind limbs on a separate treadmill belt moving at different speeds. All these examples are cases in which the normal pattern generated by the system of coupled oscillators is a stable 1:1 phase locked motion. Unfortunately, in none of the cases is it known whether the 2:1 pattern arises because of a change in the underlying oscillator frequency or in the coupling. In the sensory induced 2:1 patterns, the sensory input could be serving either to alter the coupling or to change the drive on the oscillators. Similarly, in the other examples, the two components cannot be separated adequately. We discuss here one possible model in which changes in the coupling and/or frequency differences can give rise to transitions from 1:1 to 2:1 activity in such systems (Keith and Rand, 1984).

In order to permit the model based on eqs. (3), (4) to exhibit 2:1 phase locking, we may extend the coupling to include terms of the form $h_{ij}(\theta_i,\theta_j) = h_{ij}(\theta_i - 2\theta_j)$. Specifically, we consider a system of the form:

$$\frac{d\theta_1}{dt} = \omega_1 + a\sin(\theta_2 - \theta_1) + p\sin(2\theta_2 - \theta_1) \tag{26a}$$

$$\frac{d\theta_2}{dt} = \omega_2 + a\sin(\theta_1 - \theta_2) + p\sin(\theta_1 - 2\theta_2) \tag{26b}$$

When $p = 0$ we recover the system (8) described earlier which has been shown to exhibit 1:1 phase-locked motions if the absolute value of $(\omega_1 - \omega_2)/2a$ is less than unity (cf. eq. (11)).

When $a = 0$, it may be shown that (26) can exhibit 2:1 phase-locking by letting $\psi(t) = \theta_1(t) - 2\theta_2(t)$. Then subtracting twice (26b) from (26a) gives:

$$\frac{d\psi}{dt} = (\omega_1 - 2\omega_2) - 3p\sin\psi \tag{27}$$

FIGURE 17. 2:1 activity following a medial lesion in a lamprey spinal cord.

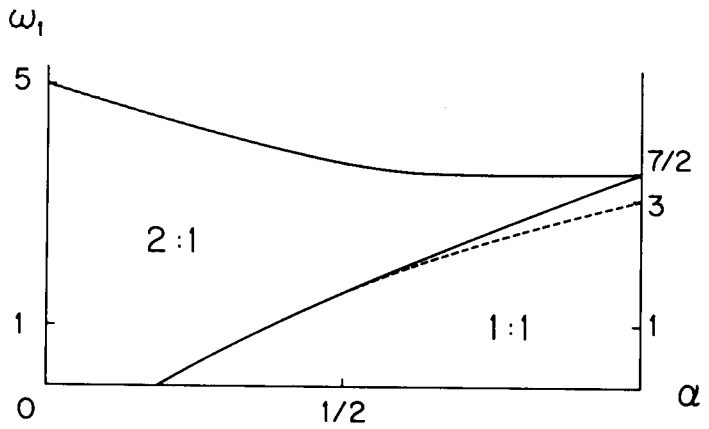

FIGURE 18. Regions of 1:1 and 2:1 phase entrainment for eqs. (34) with $p = 1 - a$ and $\omega_2 = 1$. From Keith and Rand, 1984.

2:1 phase-locked solutions correspond to equilibria of (27), since if $d\psi/dt$ is identically zero, then $d\theta_1/dt$ is twice $d\theta_2/dt$. Thus (27) exhibits 2:1 locking whenever the absolute value of $(\omega_1 - 2\omega_2)/3p$ is less than unity.

When neither a nor p are zero, eqs. (26) are more difficult to treat. Using numerical integration as well as various analytical methods, it has been shown (Keith and Rand, 1984) that as one sweeps across a parameter space defined by setting $p = 1 - a$ and $\omega_2 = 1$, there is a wide range of values for which the system (26) is 1:1 or 2:1 phase-entrained (Fig. 18).

Here we must distinguish between 1:1 *phase-locking*, in which the two phases are linearly related, i.e., $\theta_2(t) \equiv \theta_1(t)$ plus a constant, and 1:1 *phase-entrainment*, in which θ_2 completes one cycle in the same time that θ_1 does, but not necessarily by maintaining a constant phase difference. The distinction between phase-locking and phase-entrainment can be illustrated by reference to the phase torus in Figure 19.

Now let us consider the results displayed in Figure 18. The 1:1 phase-entrained region includes the points $\omega_1 < 3$, $a = 1$ (for which 1:1 locking occurs), while the 2:1 region includes the points $\omega_1 < 5$, $a = 0$ (for which 2:1 locking occurs). Both regions extend far from their respective locked states, however, showing that it is possible to obtain 2:1 entrainment under a broad range of conditions. These even include an uncoupled frequency ratio of 1:1. In the neighborhood of $a = 1$, the 2:1 region grows out of a 2:1 drift state at $\omega_1 = 7/2$, $a = 1$, into a wedge-shaped region.

Of mathematical interest is the nature of the bifurcation which occurs as one crosses from 1:1 to 2:1 phase entrainment. It has been shown numerically that many p:q phase-entrained motions occur, where p/q lies between 1 and 2. On the basis of general dynamical theory (called circle maps), it is conjectured that in fact all rational p/q between 1 and 2 occur for small open sets of parameter values between the 1:1 and 2:1 regions.

The biological significance of this work lies in the relationship between the parameter variation and the kind of phase-entrainment that the system sees. Unfortunately for the analysis of the CPGs, until more is known about the underlying mechanisms governing CPGs and their coordinating systems, the models will be helpful only in so far as they delineate the possibilities. These are many, but the modeling will be unable to differentiate between the options since it is possible to induce 2:1 entrainment in this system by changing either the coupling between the oscillators or their uncoupled frequencies.

9 CONCLUSIONS

Although we have made only modest progress towards the goal of obtaining a general theory of coupled oscillators, we have, nevertheless, provided the biological researcher with a model of coupled oscillators which may be adapted to a wide variety of applications. The model has been shown to be able to account for phase and frequency-locking in a system of N oscillators, and it offers predictions as to which parameters are important in achieving such steady states. By extending the model to include such details as double chains, second-nearest neighbor coupling, and 2:1 entrainment, we are able to further assess the importance of these parameters in particular applications. We look forward to the continued development of this approach, as we feel that the dynamics which it supports is very rich and largely uninvestigated at the present time.

ACKNOWLEDGMENTS

The authors would like to thank Nancy Kopell for several extremely useful discussions and critical comments on the manuscript. The work reported here was partially funded by the following grants, NIH: NS16803 and NSF: CME84-02069.

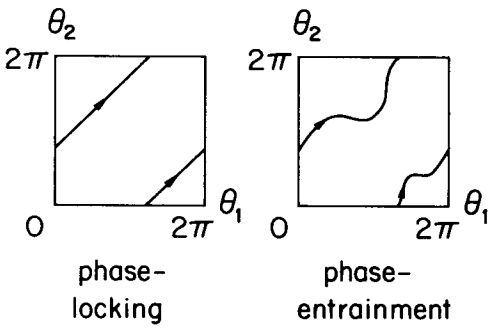

FIGURE 19. Distinction between 1:1 phase-locking and 1:1 phase-entrainment.

APPENDIX: CONTINUUM MODEL

In any real biological system, N, the number of oscillators, will always be finite. Nevertheless, we have found it useful to pass to the continuum limit by letting N approach infinity mathematically. A syncytium of neurons, or a group of neurons tightly coupled electrically, which were all endogenous oscillators would come close to this, but would still not precisely reflect the image. The continuum limit replaces the system of ordinary differential equations (ODEs) on $\varphi_i(t)$ (for example, eq. (13) or (25)), by a single partial differential equation (PDE) on $\varphi(x,t)$. That is, the continuous variable x now tags which oscillator we are interested in, whereas in the finite N case, the index i did this job. The point of this computation is that the single partial differential equation (PDE) may be easier to deal with mathematically than the system of N ordinary differential equations (ODEs).

Note that we view the continuum limit as an approximation to the more appropriate N oscillator case. This is quite the opposite of the situation in classical continuum mechanics, in which one uses finite differences to replace a PDE (considered an exact model) by a system of N ODEs (considered an approximation).

We will work with eq. (24), which includes eq. (13) as a special case. Let ℓ be the distance between two neighboring oscillators. Then as $\ell \to 0$, the differences approach derivatives as follows:

$$\frac{\theta_{i+1} - \theta_i}{\ell} \to \left.\frac{\partial \theta}{\partial x}\right|_i \quad \text{and} \quad \frac{\theta_{i+2} - \theta_i}{2\ell} \to \left.\frac{\partial \theta}{\partial x}\right|_i \tag{A1}$$

so that eq. (24) becomes

$$\frac{\partial \theta}{\partial t} = \omega(x) + a\ell \frac{\partial}{\partial x} \sin\left[\ell \frac{\partial \theta}{\partial x}\right] + 2m\ell \frac{\partial}{\partial x} \sin\left[2\ell \frac{\partial \theta}{\partial x}\right] \tag{A2}$$

Now differentiate (A2) and multiply by ℓ to get:

$$\frac{\partial \varphi}{\partial t} = \Omega(x) + a^* \frac{\partial^2}{\partial x^2} \sin \varphi + 2m^* \frac{\partial^2}{\partial x^2} \sin 2\varphi \tag{A3}$$

where $\varphi(x,t) = \ell(\partial\theta/\partial x)$, $\Omega(x) = \ell(\partial\omega/\partial x)$, $a^* = a\ell^2$, $m^* = m\ell^2$.

We are interested in steady state (phase-locked) solutions to (A3) subject to some reasonable boundary conditions, say $\varphi = 0$ at $x = 0$ and L, where L is the length of the cord. We begin by considering nearest neighbor coupling only, and we set $m^* = 0$, giving the continuum version of eq. (15):

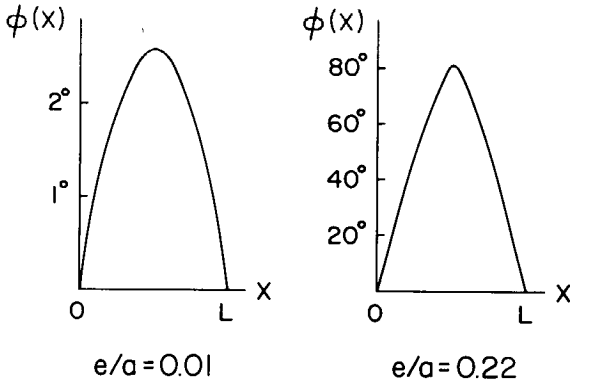

FIGURE A1. Phase difference $\omega(x)$ from continuum model with nearest neighbor coupling only, eq. (A5). In order to compare with the discrete case of N = 6 oscillators, Fig. 13, we use L/l = N and $a^* = al^2$ to obtain $eL^2/a^* = N^2e/a = 36e/a$. Since e/a = 0.01 and 0.22 in Fig. 13, we use eL^2/a^* = 0.36 and 7.92 here.

$$\sin \varphi = -\frac{1}{a^*} \iint \Omega(x)\, dx\, dx + c_1 x + c_2 \tag{A4}$$

where c_1 and c_2 are constants of integration. In order to extend the comparison, we assume that there is a constant gradient of frequencies down the system, i.e., $\Omega(x) = e$. This gives, using the boundary conditions $\varphi = 0$ at $x = 0$ and L.

$$\sin \varphi = \frac{e}{2a^*} x\,(\mathrm{L} - x) \tag{A5}$$

which is the continuum version of eq. (18), cf. Figures 13 and A1.

Now we consider the case of a continuum of identical oscillators ($\Omega(x) = 0$) with second-nearest neighbor coupling added to the foregoing case. Eq. (A3) gives, in the steady state:

$$a^* \sin \varphi + 2m^* \sin 2\varphi = c_1 x + c_2 \tag{A6}$$

Applying the boundary conditions $\varphi = 0$ at $x = 0$ and L, we obtain $c_1 = c_2 = 0$ and

$$(a^* + 4\, m^* \cos \varphi) \sin \varphi = 0 \tag{A7}$$

which has the roots

$$\varphi = 0,\ \pi,\ \arccos\left[-\frac{a^*}{4m^*} \right] \tag{A8}$$

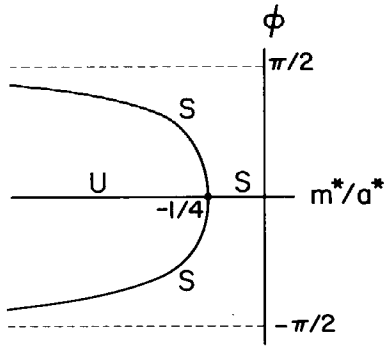

FIGURE A2. Constant phase difference φ from continuum model with nearest and second-nearest neighbor coupling, eq. (A8). The zero phase difference state is unstable for $m^*/a^* \leq \frac{1}{4}$ (U = unstable, S = stable).

These roots are displayed in Figure A2. Numerical integration of eq. (A3) for $m^*/a^* < -1/4$, $\Omega(x) = 0$, and the foregoing boundary conditions, shows that it exhibits a steady state solution which is piecewise constant in x, the solution taking on one of the values $\arccos(-a^*/4m^*)$ on each subinterval. The actual form of the piecewise constant steady state is found to be extremely sensitive to the initial conditions. In order to compare the continuum model with the finite N case of Figure 16, we set the two coupling coefficients to have equal strength, but with opposite signs, so that $m^*/a^* = -1$, and obtain the roots $\varphi = \arccos(1/4) = \pm 1.318$ radians, in approximate agreement with Figure 16.

A question was raised at the end of the section on the chain with nearest and second-nearest neighbor coupling, regarding the minimum value of inhibitory second-nearest neighbor coupling required to destablilize the zero phase difference solution of a system of N identical oscillators. We note that if the absolute value of m^*/a^* is less than 1/4, then the only roots of (A8) are $\varphi = 0$ and π. Thus the PDE suggests that the answer to the ODE question is that we require $m/a < -1/4$ to destabilize $\varphi = 0$, a result that is confirmed by numerical integration of the ODEs (25).

Before leaving the continuum model, we note that Kopell (Chapt. 10) has shown that the even function coupling terms in eq. (6) (i.e., the terms $b\,[1 - \cos(\theta_j - \theta_i)]$), play a more important role in the continuum model than do the odd terms $a \sin(\theta_j - \theta_i)$ which we have focused on in this chapter. Specifically, when the terms

$$b\,[1 - \cos(\theta_{i+1} - \theta_i)] + b\,[1 - \cos(\theta_{i-1} - \theta_i)] \tag{A9}$$

are appended to eq. (24), and the limiting processes of eqs. (A1)–(A3) are applied, there results an additional term in eq. (A3) of the form:

$$- 2b^* \frac{\partial}{\partial x} \cos \varphi \tag{A10}$$

where $b^* = bl$. In order to compare the relative importance of the even versus odd terms in eq. (6), we take $m^* = 0$ in (A3), i.e., we include only nearest neighbor coupling. Then the coefficient b^* is proportional to the small quantity l, while the coefficient a^* in (A3) is proportional to the square of l, and hence a^* is expected to be much smaller than b^* (assuming a and b are of the same order of magnitude). However, the a^* term involves a second derivative while the b^* term involves a first derivative. The net effect is to produce a *singular perturbation problem* (in the limit in which a^* is much smaller than b^*). The effect of the small second derivative terms is to produce localized boundary layers at the ends of the chain (Bender and Orszag, 1978).

REFERENCES

Abraham, R. H. and C. D. Shaw (1983). *Dynamics—The Geometry of Behavior.* Aerial Press, Santa Cruz, CA.

Bender, C. M. and S. A. Orszag (1978). *Advanced Mathematical Methods for Scientists and Engineers,* McGraw-Hill, New York.

Chay, T. R. and J. Rinzel Bursting. Beating and chaos in an excitable membrane model. *Biopys. J.* (to appear).

Cohen, A. H. (1983). Strychnine induces "fictive galloping" in the isolated spinal cord of the lamprey. *Soc. for Neurosci. Abst.*, **221**:4.

Cohen, A. H. (1984). The structure of the intersegmental coordinating system of the lamprey CPG for locomotion. *Soc. Neurosci. Abst.*, **218**:3.

Cohen, A. H. and R. M. Harris-Warrick (1984). Strychnine eliminates alternating motor output during fictive locomotion in the lamprey. *Brain Res.*, **293**:164–167.

Cohen, A. H., P. J. Holmes, and R. H. Rand (1982). The nature of the coupling between segmental oscillators of the lamprey spinal generator for locomotion: A mathematical model. *J. Math Biol.* **13**:345–369.

Cohen, A. H. and P. Wallén (1980). The neuronal correlate of locomotion in fish. "Fictive swimming" induced in an in vitro preparation of the lamprey spinal cord. *Exp. Brain Res.*, **41**:11–18.

English, A. W. and P. R. Leonard (1982), Interlimb coordination during stepping in the cat: In-phase stepping and gait transitions. *Brain Res.*, **245**:353–364.

Ermentrout, G. B. and N. Kopell (1984). Frequency Plateaus in a Chain of Weakly Coupled Oscillators, I. *SIAM J. Math. Anal.*, **15**:215–237.

Forssberg, H., S. Grillner, J. Halbertsma, and S. Rossignol (1980). The locomotion of the low spinal cat. 2: Interlimb coordination. *Acta Physiol. Scand.*, **108**:283–295.

Gambaryan, P. P. (1974). *How Mammals Run.* Halsted Press, New York.

Grillner, S. (1981). Control of locomotion in bipeds, tetrapods, and fish. In: *Handbook of Physiology.* Section 1: The Nervous System, Vol. II, Part 2. Ed. V. B. Brooks, Amer. Physiol. Soc., Bethesda, MD 1179–1236.

Grillner, S., A. McClellan, and C. Perret (1981). Entrainment of the spinal pattern generators for swimming by mechanosensitive elements in the lamprey spinal cord in vitro. *Brain Res.*, **217**:380–386.

Hildebrand, M. (1976). Analysis of tetrapod gaits: General considerations and symmetrical gaits. In *Neural Control of Locomotion*, Herman, R. H., Grillner, S., Stein, P., and Stuart, D., eds. Plenum Press, New York, pp. 203–236.

Holst, E. von (1973). *The Behavioral Physiology of Animals and Man: The Collected Papers of Erick von Holst*, vol. 1. University of Miami Press, Coral Gables.

Homma, S. and C. M. Rovainen (1978). Conductance increases produced by glycine and aminobutyric acid in lamprey interneurons. *J. Physiol. (Lond.)*, **279**:231–252.

Jacobson, R. D. and M. Hollyday (1982). Electrically evoked walking and fictive locomotion in the chick. *J. Neurophysiol.*, **48**:257–270.

Jones, A. and B. Smith (1973). Regulation of function. *J. Neurophysiol.* **27**:229–289.

Kahn, J. A. and A. Roberts (1982). Experiments on the central pattern generator for swimming in embryos of the amphibian *Xenopus laevis*, *Phil. Trans. Roy. Soc. London, Ser. B*, **296**:229–243.

Kammer, A. E. (1968). Motor patterns during flight and warm-up in Lepidoptera, *J. Exp. Biol.* **48**:89–109.

Keith, W. L. and R. H. Rand (1984). 1:1 and 2:1 phase entrainment in a system of two coupled limit cycle oscillators, *J. Math Biology*, **20**:133–152.

Kulagin, A. S. and M. L. Shik (1970). Interaction of symmetrical limbs during controlled locomotion *Biofizika*, **15**:164–170 (Engl. transl. 171–178).

Mehler, W. R. (1960). More nonsense. In *The Book*, D. Purpura and Y. Yahr, eds. Press, New York, pp. 101–110.

Neu, J. C. (1979). Coupled chemical oscillators, *SIAM J. Appl. Math*, **37**:307–315.

Neu, J. C. (1980). Large populations of coupled chemical oscillators, *SIAM J. Appl. Math.*, **38**:189–208.

Pavlidis, T. (1973). *Biological Oscillators: Their Mathematical Analysis*, Academic Press, New York.

Rand, R. H. and P. J. Holmes (1980). Bifurcation of periodic motions in two weakly coupled van der Pol oscillators *Int. J. Nonlinear Mechanics*, **15**:387–399.

Rand, R. H., D. W. Storti, S. K. Upadhyaya, and J. R. Cooke (1982). Dynamics of coupled stomatal oscillators, *J. Math. Biology*, **15**:131–149.

Rinzel, J., Bursting oscillations in an excitable membrane model. In *Proc. 8th Dundee Conf. on the Theory of Ordinary and Partial Differential Equations*, B. D. Sleeman, R. J. Jarvis, and D. S. Jones, eds. Springer Verlag, to appear.

Rovainen, C. M. (1985). Effects of propriospinal interneurons on fictive swimming in lamprey. *J. Neurophysiol.*, **54**:959–977.

Stein, P. S. G. (1978). Swimming movements elicited by electrical stimulation of the turtle spinal cord: the high spinal preparation. *J. Comp. Physiol.*, **124**:203–210.

Viala, D. and C. Vidal (1978). Evidence for distinct spinal locomotion generators supplying respectively fore- and hind-limbs in the rabbit. *Brain Res.*, **155**:182–186.

Winfree, A. T. (1980). *The Geometry of Biological Time*. Springer-Verlag, New York.

Young, R. E., J. L. Wilkens, and C. Dodd (1980). Pharmacological dissection of a neural pattern generator. *J. Comp. Physiol.*, **139**:1–10.